arXiv:1405.1839v1 [astro-ph.EP] 8 May 2014

Tidally distorted exoplanets : density corrections for short-period hot-Jupiters based solely on observable parameters

J. R. Burton[1], C. A. Watson[1], A. Fitzsimmons[1], D. Pollacco[2],
V. Moulds[1], S. P. Littlefair[3], P. J. Wheatley[2]

jburton04@qub.ac.uk

ABSTRACT

The close proximity of short period hot-Jupiters to their parent star means they are subject to extreme tidal forces. This has a profound effect on their structure and, as a result, density measurements that assume that the planet is spherical can be incorrect. We have simulated the tidally distorted surface for 34 known short period hot-Jupiters, assuming surfaces of constant gravitational equipotential for the planet, and the resulting densities have been calculated based only on observed parameters of the exoplanet systems. Comparing these results to the density values assuming the planets are spherical shows that there is an appreciable change in the measured density for planets with very short periods (typically less than two days). For one of the shortest-period systems, WASP-19b, we determine a decrease in bulk density of 12% from the spherical case and, for the majority of systems in this study, this value is in the range of 1-5%. On the other-hand, we also find cases where the distortion is negligible (relative to the measurement errors on the planetary parameters) even in the cases of some very short period systems, depending on the mass ratio and planetary radius. For high-density gas-planets requiring apparently anomalously large core masses, density corrections due to tidal deformation could become important for the shortest-period systems.

Subject headings: planets and satellites: atmospheres – planets and satellites: fundamental parameters

[1]Astrophysics Research Centre, Queen's University Belfast, Belfast, BT7 1NN, UK

[2]Department of Physics and Astronomy, University of Warwick, Coventry, CV4 7AL, UK

[3]Department of Physics and Astronomy, University of Sheffield, Sheffield, S3 7RH, UK

1. Introduction

Since the first planet outside the solar system was discovered orbiting the millisecond pulsar PSR1257+12 (Wolszcan et al. 1992), the study of extra-solar planets has rapidly become one of the key research areas in astronomy today. At the time of writing, 1782 exoplanets have been identified through many different techniques including radial velocity measurements, gravitational microlensing, transit surveys and many others. As of writing, 1133 are known to be transiting, mostly discovered by transit surveys such as SuperWASP (Pollacco et al. 2006), CoRoT (Borde et al. 2003), the HATnet project (Bakos et al. 2002) and Kepler (Boricki et al. 2010). Transiting systems provide a radius, and hence bulk density when coupled with the planetary mass determined from radial velocity follow-up, as well as characterising their atmospheres with techniques such as transmission spectroscopy (Charbonneau et al. 2001, Snellen et al. 2008) and secondary eclipse photometry (Gibson et al. 2010, Burton et al. 2012). The bulk density is an important parameter to determine, as this value is used in chemical composition models and atmospheric simulations. The bulk density is measured by determining the radius of the planet from the transit lightcurve, and assuming a spherical planet in order to work out the volume. Since the volume and mass of the planet are then both known, a simple bulk density calculation can be applied.

Previous work on modelling exoplanet distortion has been carried out by Leconte et al. (2011), who demonstrated that tidal and rotational forces result in a systematic underestimation of the planetary radius. The tidal distortion is particularly relevant for short period planets with low masses and large radii, as these systems are subject to a significant amount of gravitational interaction with the host star. Since the bulk of the distortion would lie along the axis connecting the star and planet, this effect would not be apparent during transit observations – where the planet will appear largely spherical due to the observer being presented with a smaller cross-sectional area during transit. Failing to account for this distortion would therefore result in a systematic overestimation of the measured densities of exoplanets, since the volume is calculated based on the planet being spherical. Since a significant proportion ($\sim$30%) of exoplanets so far discovered have orbital separations of $\lesssim$0.1A.U. (Matsumura et al. 2010), this could potentially affect the measured bulk densities of a number of hot-Jupiter systems. Indeed, work by Lammer et al. (2009) and Li et al. (2010) show that distortion in WASP-12b is appreciable, and can potentially impact on mass-loss rates for short-period systems. Naturally, if the tidal forces are weak, the distortion will be negligible, and the planet remains close to spherical.

While Leconte et al. are able to calculate the distorted shapes of exoplanets, which has important implications for our understanding of the internal dynamics of short period sys-

tems, their approach is limited in that the models are difficult to reconcile with observational parameters. For example, the work of Leconte et al. requires detailed internal structure models, incorporating effects such as rotation and atmospheric structure. These parameters are obtained from models derived from measurements of Jupiter and Saturn. Since our Solar System's gas giants have markedly different rotation periods, orbital separations and incident fluxes to those of the short-period hot-Jupiters, accurate determination of such internal parameters for hot-Jupiters is fraught with uncertainty and potential error, as well as being beyond the expertise of the average observer. This is further demonstrated by the fact that, to the best of our knowledge, the important work by Leconte et al. has never been applied to determine planetary density corrections in any observational exoplanet characterisation publication (though it has been used to indicate the importance of tidal distortion effects e.g. Mancini et al. 2013, Kovacs et al. 2013). The aim, therefore, was to outline a much simpler model to estimate planetary distortion, which would be easier to implement and would be comparable to the more detailed simulations of Leconte et al. In order to make the models as applicable to observers as possible, the main focus of the modelling was to estimate the distortion using observed parameters gleaned from transit photometry and RV measurements.

In this paper, we model the gravitational interaction between the parent star and planet using the Roche approximation, and show that tidal distortion can be significant for hot-Jupiters with orbital periods less than $\sim$2 days. In section 2, we outline the method of constructing a distorted hot-Jupiter and measuring the volume in order to work out the change in bulk density, and use this model in section 3 to estimate the distortion of hot-Saturn-like planets. In section 4, we use the parameters of the shortest-period systems, derived from follow-up photometry and radial-velocity measurements, to calculate the tidal distortion of these exoplanets, and discuss the significance of these findings, comparing the results with the simulations by Leconte et al.

2. Method

In order to model the exoplanets' tidally distorted surface, we have assumed that it lies along a surface of constant gravitational potential. Under the Roche approximation (Chandrasekhar 1969), the total gravitational potential (Φ) at any point within the system is given by;

$$\Phi = -\frac{GM_1}{(x^2+y^2+z^2)^{1/2}} - \frac{GM_2}{[(x-a)^2+y^2+z^2]^{1/2}} - \frac{1}{2}\Omega^2[(x-\mu a)^2+y^2], \quad (1)$$

(e.g. Pringle 1985) where M_1 is the mass of the primary component (in this case the host star) and M_2 is the mass of the secondary (in this case the exoplanet). x, y and z are co-ordinates in which the surface is plotted with the origin at the centre-of-mass of the primary component, where x is along the line-of-centre, y is along the orbital plane and z makes a right-handed set. a is the orbital separation between the centres-of-mass of the two components. $\mu = \frac{M_2}{M_1+M_2}$ and $\Omega = \frac{2\pi}{P_{orb}}$ (the angular velocity of the system), where P_{orb} is the orbital period.

The Roche approximation has widely been used to model interacting binary systems, such as Cataclysmic Variables (CVs). For example, Roche tomography (for a description, see e.g. Rutten et al. 1996, Watson et al. 2004) uses the Roche approximation in order to reconstruct the surface features of secondaries for a number of CV systems from the velocity profiles (Watson et al. 2001, Watson et al. 2003, Dunford et al. 2012). Given the extreme tidal forces acting on some short period hot-Jupiters, it was decided to model their shapes using the Roche approximation. The main advantage of this approach is that it is possible to obtain the distortion solely from the observed system parameters as opposed to methods which use parameters derived from simulations, such as planetary rotation and internal structure. We note here that the Roche approximation has previously been used by Budaj (2011) to estimate the reflection effect for tidally distorted planets, but density corrections were not calculated for these systems.

In order to measure the distortion of the planet using the Roche approximation, a number of assumptions have been made. First, we have assumed the planet is tidally locked with the star, so the orbital period is equal to the rotation period. We also assume the orbit has been circularised, so as to keep the distortion over the orbital period constant. This is a reasonable assumption, as it follows predictions of hot-Jupiter formation and follow-up work (e.g. Nagasawa et al. 2008). It is also a requirement of equation 1. We have also assumed that the mass of the planet is centrally condensed, again, required by equation 1. This was also an assumption made by Leconte et al. and, for example, simulations by Campo et al. (2010) predict a centrally condensed WASP-12b given an orbital eccentricity of $\sim$0.

In order to match the model to the observed radius, the value of Φ in equation 1 was adjusted such that the projected area of the model planet during transit matched those

given by observations. This method gives the quantity $(R_P/R_S)^2$, the ratio of the planetary occulting area to projected star area. Since this is equivalent to the actual parameter derived from the transit light curve, this was determined to be the best method in which to set the value of R_P, as opposed to just setting the value of Φ to return the corresponding polar radius. The three-dimensional output is given in Figure 1, along with the spherical case using the parameters of WASP-19, a planetary system with one of the shortest known orbital periods (0.79 days). Figure 2 shows the sky-projected surface area of WASP-19b for both the spherical and distorted case at phase 0. As can be seen from the projections, the polar radius at zero phase is almost identical. This is due to the bulk of the distortion being projected away from the observer, towards the star, making the planet appear spherical in both cases.

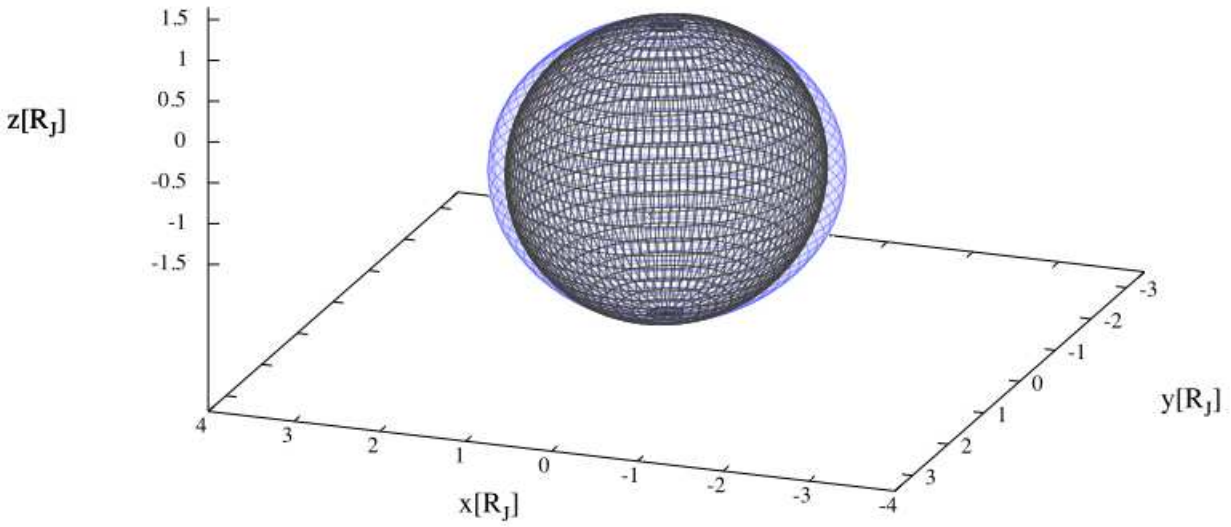

Fig. 1.— The surface of WASP-19b at quadrature for both the spherical case (black line) and distorted case (blue, or light grey line), viewed slightly above the orbital plane for clarity. Note how the distorted case is more oblate, and the increase in volume is appreciable.

Since the precise co-ordinates of the tiles were known, the volume of each 'slice' of elements was determined by finding the area bounding the surface of the tile with the centre of the slice. The area was then multiplied by the depth of each slice, effectively modelling it as a tapered wedge. The number of tiles were set sufficiently high to make the gaps

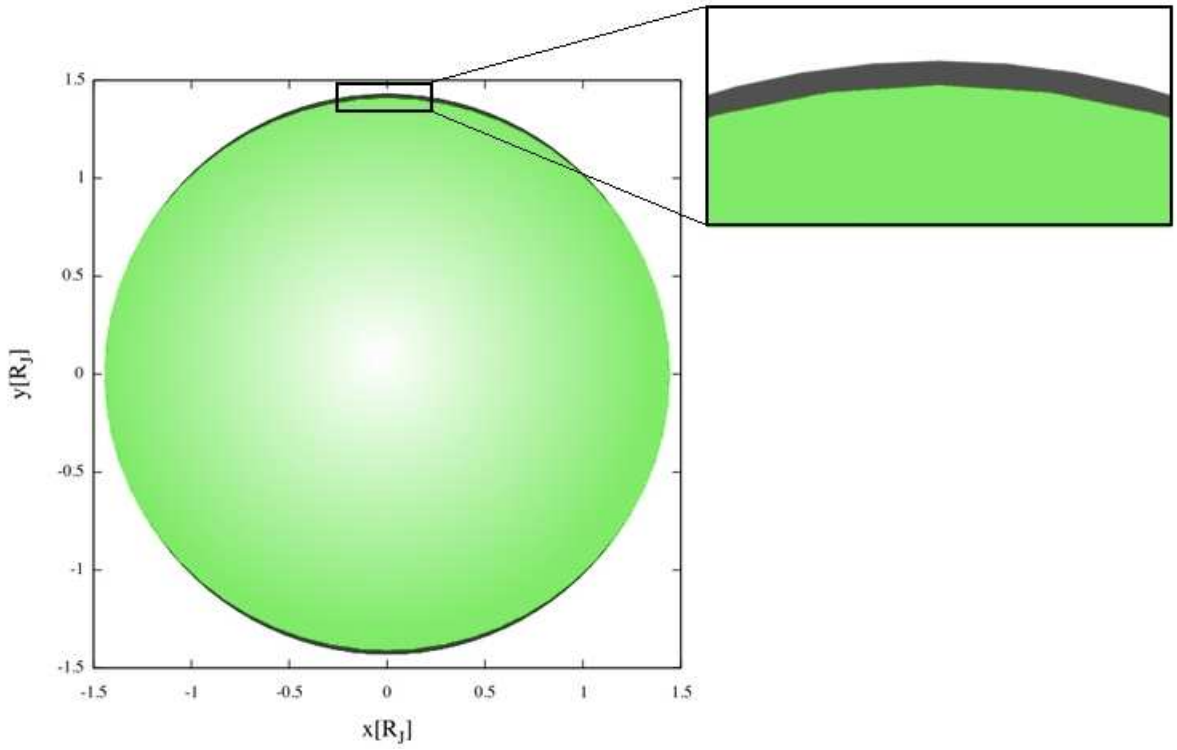

Fig. 2.— The sky projected surface of equal area of WASP-19b at zero phase for both the spherical case (black) and distorted case (green/light grey). It can be seen that the distorted case is very close to the spherical case, and thus the distortion will be extremely difficult to detect during transit.

between sequential tile areas negligible, but also sufficiently low to avoid truncation issues when working out the projected area. To check there were no jumps in the projected area due to the tile projections, the density of the planet was calculated as a function of orbital period. Figure 3 is an example of this process using the system parameters of WASP-19b.

This allowed for the internal consistency of the code to be tested by setting the orbital period of the system to a value where one would expect the distortion to be negligible, and hence the planet to be spherical. At around 10 days, the difference between the volume given by the spherical case and the volume output from the simulations was $\sim$0.001% for WASP-19b. Once the accuracy and consistency of the code had been thoroughly established and tile truncation and placement errors had been minimised, the parameters of thirty-four short-period hot-Jupiters were obtained in order to model the tidal distortion for each of these systems. We discuss the impact of this in section 4.

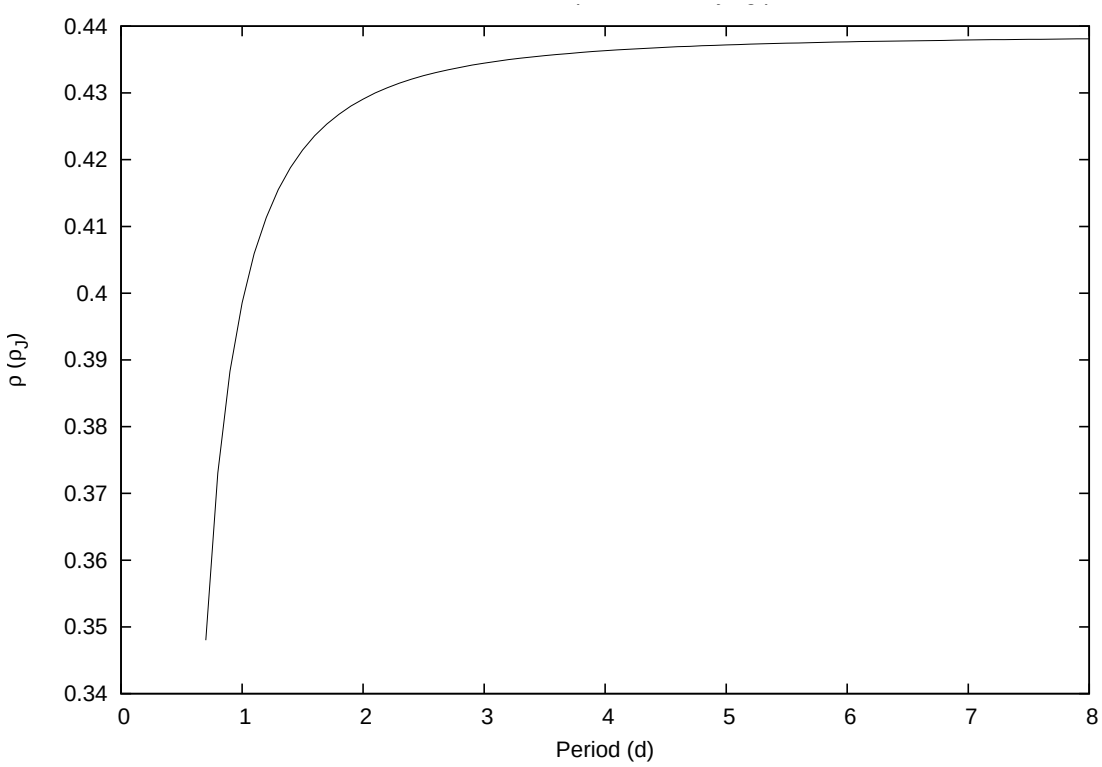

Fig. 3.— Change in bulk density as a function of orbital period using the parameters of WASP-19b. After approximately 2 days, the change is negligible when compared to the density at the actual period of 0.7888 days.

3. Saturn-like planets

As a final demonstration, a number of cases of exoplanets with parameters similar to Saturn have been modelled with the orbital period set to one day, the results of which are summarised in Table 1. This was carried out in order to investigate the region of planetary parameters, primarily star-to-planet mass ratio, which are most susceptible to a severe (i.e. >20%) level of distortion. A $1M_J$ model and 0.3 M_J (Saturn-like) model have been added as a comparison. We have also run the simulations over a range of orbital periods. The results from these simulations indicate that for Saturn-mass planets, the density correction is significantly important for orbital periods of less than ∼1.5 days. For a hot-Saturn with an orbital period of 0.6 days, the density correction approaches 25%, sufficient to alter the position of the exoplanet on the mass-radius relation (see Figure 5). Whilst there has yet to be a candidate discovered matching these orbital parameters, many systems are being identified with densities matching that of Saturn with short orbital periods (e.g Fortney et al. 2011, Ojeda et al. 2013, Gandolfi et al. 2013). It can be seen that a density correction of ∼5-

10% is being approached for systems with more massive host stars, for orbital periods of 1 day. Whist systems matching these exact parameters have yet to be discovered, hot-Jupiters with orbital periods of less than one day are known to exist (e.g. WASP-18b, WASP-19b, CoRoT-7b, Kepler-10b, Kepler-70b). The parameters we have used for these simulations provide an initial, if somewhat speculative, investigation into planets which could potentially show extreme levels of distortion. In the case of GJ163b – a non-transiting exoplanet – we have simply used the mass ratio of the system with a Saturn-like radius, as the radius of the planet cannot be constrained from radial velocity measurements.

An especially interesting case is that of HD149026b. Since its discovery in 2005, the incredibly high density (1.17gcm^{-3}) has resulted in the prediction of an anomalously high core mass of 70-85$M_{\oplus}$ (Sato et al. 2005). Previous predictions of planetary formation using the core accretion model indicate a maximum core mass of 30$M_{\oplus}$ before runaway gas accretion occurs (Ikoma et al. 2006). Several explanations for the massive core of HD149026b have been proposed, including heavy element rain onto the core, accretion of planetesimals and collisions between planetary embryos (Sato et al. 2005; Fortney et al. 2006). While the gravitational distortion of this planet with its current orbital period of 2.8 days is insufficient to lower its density in order to reduce the core mass to levels that agree with accretion theory, gravitational distortion could allow this for shorter period systems, should they be observed. For example, a Saturn-mass planet in a 1 day orbit around a 1.1$M_{\odot}$ star would yield a radius of 0.7R_J if sphericity was assumed, but would actually have a mean radius closer to 0.8R_J due to gravitational distortion. Using the evolutionary models of Bodenheimer et al. (2003) in addition to the core mass values calculated by Sato et al. (2005) with our new density value would allow a more accurate core mass to be estimated for such systems. For the case above, assuming a spherical planet (i.e. a radius of 0.7R_J), the core mass would be calculated to be 85$M_{\oplus}$ assuming a core density of 5.5gcm^{-3}, and a core mass of $<$74$M_{\oplus}$ assuming a core density of 10.5gcm^{-3} (the core density of Saturn). The value of our density correction, however, would result in a corrected estimate of the core mass of $<$74$M_{\oplus}$ assuming a core density of 5.5gcm^{-3}, and a core mass of $<$60$M_{\oplus}$ assuming a core density of 10.5gcm^{-3} for the distorted case. This reduction in the core mass of a planet analogous to HD149026b on a sufficiently short-period indicates that hot-Saturns discovered to have a higher than expected core mass can be partially explained by the tidal distortion effect. Additional mechanisms, such as accretion of planetesimals, can then be invoked to explain this much more easily with a reduced core mass.

Table 1: Output from simulations using the mass-ratios of three exoplanet systems, HD149026, WASP-29 and GJ163, using a 1 day orbital period. Also included as a comparison are the cases for a Jupiter-mass planet and a Saturn-mass planet orbiting a $1M_{\odot}$ star with a period of 1 day. The density values have been indicated for both the spherical (6) and distorted cases (7).

System	M_S ($M_{\odot}$)	M_P (M_J)	R_P (R_J)	Ref.	ρ_{sph}	ρ_{1d}	$\Delta\rho$
(1)	(2)	(3)	(4)	(5)	(6)	(7)	(8)
Model hot-Jupiter	1.0	1.0	1.0	-	0.238	0.229	3.0%
Model hot-Saturn	1.0	0.3	0.8	-	0.186	0.172	7.5%
HD149026b	1.3	0.356	0.718	[1]	0.229	0.210	8.25%
WASP-29b	0.825	0.244	0.792	[2]	0.117	0.108	7.85%
GJ163b	0.4	0.354	0.8*	-	0.156	0.163	4.47%

[1] Southworth (2010) [2] Hellier et al. (2010)

* Since this candidate is not a transiting planet, only the mass has been constrained from radial velocity measurements. For this planet, a radius comparable to that of Saturn has been assumed.

4. Results and discussion

The results for thirty-four short-period hot-Jupiters are shown in Table 2. The most significant distortion of the hot-Jupiters modelled occur for the shortest period systems, with WASP-19b having a density which is 12% less than the spherical case. Since the size of the Roche lobe is dependent on the period (and thus the separation distance of the components) in addition to the mass ratio of the two components, this follows expectations. However, WASP-43b also has an extremely short period, and one therefore might expect a distortion comparable to that of WASP-19b or WASP-12b ($\sim$11%). Whilst the period is a key parameter in the size of the critical Roche lobe, in the case of WASP-43b the density is extremely high (over twice that of Jupiter). This means that for the mass ratio of this system, combined with the relatively small radius of the planet, the distortion due to tidal interactions for this system is negligible, at least in comparison with systems with a similar orbital period. Essentially, for planets with a large mass ($>1.5M_J$), but with a radius comparable to that of Jupiter, the distortion is negligible for a given stellar mass. Again, this follows expectations, since the critical Roche lobe is much bigger and, as a consequence, the planet has very little distortion as it lies well within its Roche lobe. This can be seen for planets such as Corot-14b and WASP-14b. Also, for planets, with an orbital period of greater than $\sim$2 days, the distortion becomes negligible as is also evident in Figure 3. The other main variable which causes a similar change in the size of the Roche lobe is the mass ratio of the two components. For a more massive host star, the size of the critical Roche lobe decreases. Conversely, a

more massive planet will allow for the size of the Roche lobe to increase, however in the case of the extreme mass ratio between a host star and planet, this effect is much less significant than for example in CVs, where the mass of the components is comparable. For the planets we have investigated, the mass ratio of the systems is relatively uniform, as indicated in Figure 4 and Table 2. However, given the extreme mass ratio between hot-Jupiter and host star (of the order $\sim 10\times^{-3}$), this parameter value is a very important determining value as to the distortion of the exoplanet. For the majority of systems we have modelled, the change in bulk density from the spherical case is in the range 1-5%, meaning that even for systems where the parameters are not particularly conducive to a major distortion, this effect can still be significant. It should be noted that typical measurement uncertainties on the masses and radii of exoplanets (and their host stars) lead to errors on the derived bulk densities of the order of ∼5%. Thus, for the majority of the systems in Table 2 the correction required is not significant – and only the most heavily distorted planets present a significant level of bulk density correction. In the specific case of WASP-19b, for example, the measurement error on the currently published bulk density is 6.1% (Hellier et al. 2011a) – significantly less than the correction needed to account for tidal distortion (12.0%). In addition, it should be noted that the distortion effect is systematic in that it can only decrease the density. In the future, as measurement errors on the radius and mass of the systems are refined, the bulk density error value/distortion will become more important. Figure 4 shows the decrease in bulk density as a function of orbital period for these planets from Table 2. The radius of the hot-Jupiter is represented by the size of the points on the graph. As expected, the shortest period hot-Jupiters are the most susceptible to tidal deformation, leading to overestimates of the planetary density of >10% in some cases.

The results from our simplified Roche models agree with the more complex approach of Leconte et al.. The two cases of particular interest being the two most distorted exoplanets we modelled; WASP-12b and WASP-19b. Leconte et al. return a radius increase in the direction of the distortion of 3% for WASP-12b and 2.72% for WASP-19b, in comparison with our volume calculations which return an increase of 3.21% and 3.56%, respectively. These figures are likely to change as the error bars on the observed parameters are refined, and the difference between the radius values calculated from simulations (as used by Leconte et al.) and the simpler Roche method should be compared when new volume models are generated. It is also mentioned by Leconte et al. that WASP-12b will have a mean density decrease of ∼9% based on their calculations, again, in close agreement with our value of 11%. The models described in this paper provide observers with a fast and simple estimation of the distortion, without the need to invoke estimations of uncertain internal parameters such as rotation rates, or requiring the user to calculate complex internal structure profiles. Indeed, recent observations by Sing et al. (2013) have indicated that WASP-12b has a density ∼20%

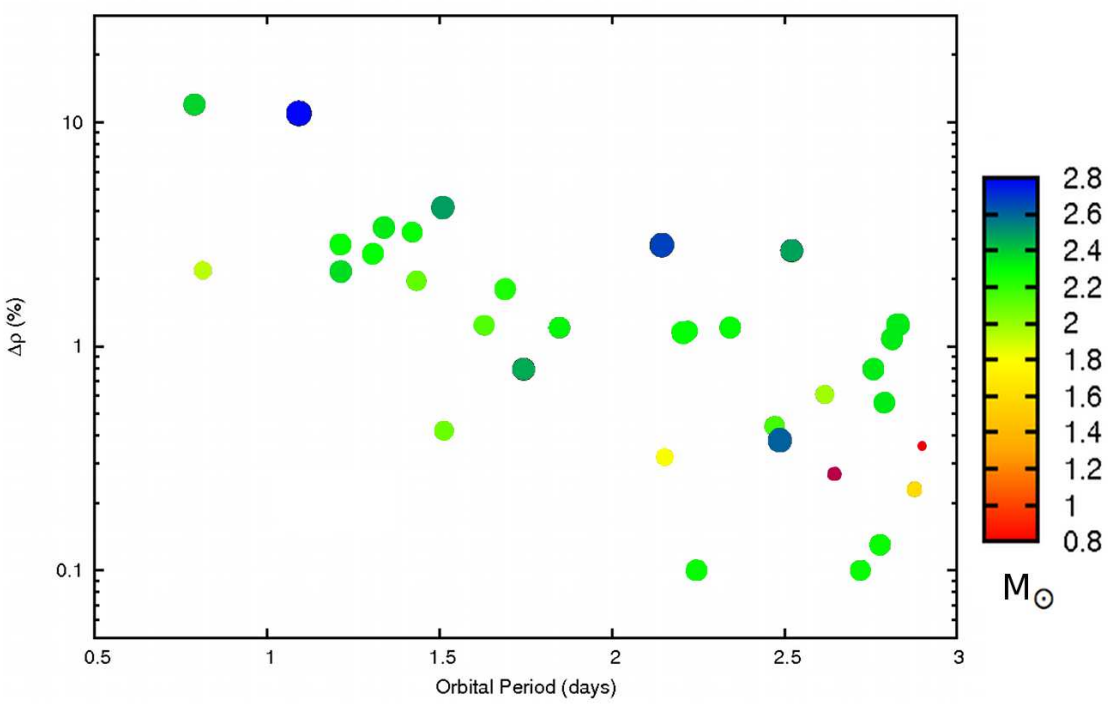

Fig. 4.— The decrease in bulk density on a logarithmic scale as a function of orbital period for the selection of short-period hot-Jupiters from Table 2. As expected from the Roche approximation (equation 1), as the orbital period increases, the density correction decreases. The respective size of the circles represent the radius of the planet, and the colour gradient represents the mass of the host star.

lower than previously estimated. By comparing the results from our model with observations such as these, we will be able to improve the accuracy of the density correction estimation by adding effects such as mass loss during subsequent iterations.

We must also consider the limitations of using this technique to model the distortion. As previously mentioned, equation 1 assumes orbital circularisation, and while this is a reasonable assumption, two of the planets considered in this work have significant eccentricities. HAT-P-23b and GJ436b both have $e{\sim}0.1$, meaning the method used for these systems is not strictly applicable, and the density changes for these planets will differ from the stated amounts. For GJ436, this is not much of an issue, as the spherical density of this planet is already high ($>1.5\rho_J$), and the distortion given its 2.64-day period will not be significant. However, for systems with periods comparable to that of HAT-P-23b (1.2 days) and with appreciable eccentricities, the method we have used will produce a density change which is

likely to be incorrect. The system components are also assumed to be centrally condensed. Again, while this is a reasonable assumption, work carried out by Sirotkin et al. (2009) indicates that the internal structure of low mass CV donors deviate from this assumption, resulting in slightly different Roche-volumes on the level of a few percent. While the models we have constructed do not fill the critical Roche lobe, this is nevertheless an important effect, as planets with a sufficiently high density only have a volume increase on the level of 0.5-1%.

As stated by Li et al. (2010), the light curve from a tidally-distorted hot-Jupiter would be different from the spherical case. Simulations indicate that at the quarter and three-quarters phase, the flux would be $\sim$10% greater due to the effective area being greater. Sufficient observations of day-night variations in the infra-red could, in theory, be able to detect this. However, since the change in intensity is almost beyond detection limits for ground-based platforms, space-based observations would be the ideal approach to detect the distortion (e.g. Spitzer, Hubble). In addition, oblateness of a transiting exoplanet would reveal itself through slight anomalies in ingress and egress. Carter et al. (2009) used Spitzer photometry to place oblateness constraints on the hot-Jupiter HD189733, concluding it is less oblate than Saturn. This is to be expected, however, as the spin rate for hot-Jupiters are expected to have been slowed due to tidal friction into synchronous orbit. It has also been shown that this effect is extremely difficult to measure, even for hot-Jupiters with periods of less than two days (Carter et al. 2010). From Figure 1, when viewed from the quarter-phase position, the distortion of the planet does indeed appear appreciable. Figure 2, however, shows the distortion at 90° inclination and zero phase. From this angle, the two cases are remarkably similar, indicating that even for planets with an appreciable distortion the oblateness is not particularly significant, in agreement with Carter et al. (2010).

Given the likely over-estimation of the density of short-period hot-Jupiters as currently reported, there may also be an impact on current atmospheric simulations, as the species of molecule composing the upper atmosphere is dependent on the overall density. For example, Adams et al. (2008) and Swift et al. (2012) show that for a given mass-radius relation, the exoplanet's bulk composition can be found. However, the bulk composition is insensitive to a change in mass for planets greater than $\sim$100 Earth masses ($\sim 0.3 M_J$) but is still sensitive to a change in effective radius. Mass-density plots, such as those provided in Szabó et al. (2011) for transiting exoplanets will also require an adjustment factor for the lower-mass hot-Jupiters. A change of 10% of the volume of a planet may allow for the planet to move from a bulk composition of H/He to one of H alone. Simulations indicate that a Saturn-mass planet with a radius of $\sim 1 R_J$ would have a volume 10% greater than an assumed spherical planet on a 1.5-day-period, meaning that for hot-Saturns, a shift in the bulk composition is possible. Figure 5 shows an example of the mass-radius parameter space from Swift et al.

(2012) highlighting the particular area of interest which would result in a potential impact on composition simulations.

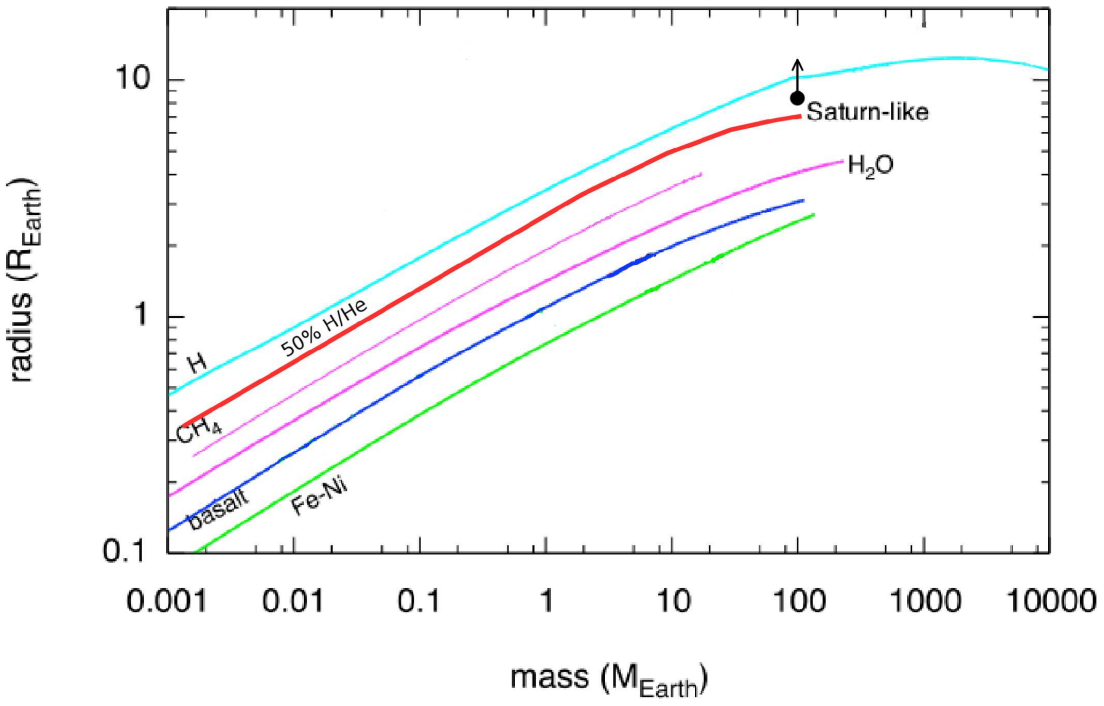

Fig. 5.— Mass-radius relations for a number of different compositions from Swift et al. (2012). The 50% H/He line (red curve) has been added from Sasselov (2008). The arrow represents the magnitude by which the tidal distortion can alter the radius from the spherical case.

5. Conclusions

The tidal forces short-period exoplanets are subject to due to gravitational interactions with the host star can result in an appreciable decrease in the bulk density once this effect is accounted for. Due to the bulk of the distortion being along the axis connecting the centres-of-mass, this distortion is not apparent during transit, and hence when the density of the planet is being measured, this effect is not accounted for. For the most distorted systems, the corrected bulk densities could cause the assumed bulk composition to change, meaning

atmospheric simulations must take this into account when dealing with short-period systems, as well as for planets with a low mass/radius ratio.

We have demonstrated that for short-period systems, the decrease in bulk density from the spherical case is of the order of 10% for systems where the parameters allow for the most distortion. It has also been shown that for particularly dense planets, this effect is negligible, even for systems with periods less than one day. As further exoplanets are discovered, the mass-ratio of these systems will also provide a further census of planets with more extreme mass ratios where the gravitational distortion will be enhanced. The method we have used matches previous models based on much more complex internal modelling of the planet as a whole, and provides a simple method for observers to estimate the distortion limits. As more hot-Jupiters with even more extreme environments are being discovered, it is imperative that any correction in the parameters obtained for these systems are applied in order to obtain the most accurate possible atmospheric models. In addition, modelling hot-Saturn planets can also provide important information for internal modelling simulations, as in the case of a short-period planet with parameters similar to HD149026b.

Acknowledgements

JB is funded by the Northern Ireland Department of Employment and learning, and in addition would like to thank C Walsh, M Fraser and M McCrum for useful discussion.

REFERENCES

Adams, E. R., Seager, S., Elkins-Tanton, L. 2008, ApJ, 673, 1160

Alonso, R., Auvergne, M., Baglin, A., Ollivier, M., Moutou, C. et al. 2008, A&A, 482, L21

Alsubai, K. A., Parley, N. R., Bramich, D. M., West, R. G., Sorensen, P. M. et al. 2011, MNRAS, 417, 709

Bakos G. A., Lazar J., Papp I., Sari P. & Green E. M. 2002, PASP, 114, 974

Bakos, G. Á., Shporer, A., Pál, A., Torres, G., Kovács, G. et al. 2007, ApJ, 671, L173

Bakos, G. Á., Hartman, J., Torres, G., Latham, D. W., Kovács, G. et al. 2011, ApJ, 742, 116

Barge, P., Baglin, A., Auvergne, M., Rauer, H., Léger, A. et al. 2008, A&A, 482, L17

Bodenheimer, P., Laughlin, G., Lin, D. N. C., 2003, ApJ, 592, 555

Bordé P., Rouan D. & Léger A. 2003, A&A, 405, 1137

Borucki W. J., et al. 2010, Science, 327, 977

Buchhave, L. A., Bakos, G. Á., Hartman, J. D., Torres, G., Kovács, G. et al. 2010, ApJ, 720, 1118

Budaj, J. 2011, AJ, 141, 59

Burke, C. J., McCullough, P. R., Valenti, J. A., Johns-Krull, C. M., Janes, K. A. et al. 2007, ApJ, 671, 2115

Burton, J. R., Watson, C. A., Littlefair, S. P., Dhillon, V. S., Gibson, N. P et al. 2012, ApJS, 201, 36

Campo, C. J., Harrington, J., Hardy, R. A., Stevenson, K. B., Nymeyer, S. et al. 2010, ApJ, 727, 125

Carter, J. A., Winn, J. N., Gilliland, R., Holman, M. J. 2009, ApJ, 696, 241

Carter, J. A. & Winn, J. N. 2010, ApJ, 709, 1219

Charbonneau, D., Brown, T. M., Noyes, R.W. & Gilliland, R. L. 2001, AJ, 568, 377

Chandrasekhar, S. 1969, The Silliman Foundation Lectures, New Haven: Yale University Press

Christiansen, J. L., Ballard, S., Charbonneau, D., Deming, D., Holman, M. J. et al. 2011, ApJ, 726, 94

Dunford, A., Watson, C. A., Smith, R. C. 2012, A&A, 525, A140

Ehrenreich, D., Lecavelier Des Etangs, A., Hébrard, G., Désert, J. M., Vidal-Madjar, A. et al. 2008, A&A, 483, 933

Enoch, B., Anderson, D. R., Barros, S. C. C., Brown, D. J. A., Collier-Cameron, A. et al. 2011, AJ, 142, 86

Fortney, J. J., Saumon, D., Marley, M. S., Lodders, K., Freedman, R. S., 2006, ApJ, 642, 495

Fortney, J. J., Demory, B.-O., Désert, J.-M., Rowe, J., Marcy G. W. et al. 2011, ApJS, 197, 9

Gandolfi, D., Parviainen, H., Fridlund, M., Hatzes, A. P., Deeg, H. J. et al. 2013, A&A, 557, A74

Gibson, N. P., Aigrain, S, Pollacco, D. L., Barros, S. C. C., Hebb, L. et al. 2010, MNRAS, 404, L114

Gillon, M., Pont, F., Moutou, C., Bouchy, F., Courbin, F. et al 2006, A&A, 2006, 459, 249

Gillon, M., Hatzes, A., Csizmadia, S., Fridlund, M., Deleuil, M. et al. 2010, A&A, 520, A97

Hebb, L., Collier-Cameron, A., Loeillet, B., Pollacco, D., Hébrard, G. et al. 2009, ApJ, 693, 1920

Hellier, C., Anderson, D. R., Collier-Cameron, A., Gillon, M., Lendl, M. et al. 2010, ApJ, 723, L60

Hellier, C., Anderson, D. R., Collier-Cameron, A., Miller, G. R. M., Queloz, D. 2011, ApJ, 730, L31

Hellier, C., Anderson, D. R., Collier-Cameron, A., Gillon, M., Jehin, E. et al. 2011, A&A, 535, L7

Ikoma, M., Guillot, T., Genda, H., Tanigawa, T., Isa, S., 2006, ApJ, 650, 1150

Johnson, J. A., Winn, J. N., Bakos, G. Á., Hartman, J. D., Morton, T. D. et al. 2011, ApJ, 735, 24

Joshi, Y. C., Pollacco, D. L., Collier-Cameron, A., Skillen, I., Simpson, E. et al. 2009, MNRAS, 392, 1532

Kovács, G. et al. 2013, A&A, 553, A44

Lai, D., Rasio, F. A., Shapiro, S. L. 1994, ApJ, 423, 344

Lammer, H., Odert, p., Leitzinger, M., Khodachenko, M. L., Panchenko, M. et al. 2009, A&A, 506, 399

Leconte, J., Lai, D., Chabrier, G. 2011, A&A, 2011, 528, A41

Li, S., Miller, N., Douglas, N., Lin, C. & Fortney, J. J. 2010, Nature, 463, 1054

Mancini, L. et al. 2013, A&A, 551, A11

Matsumura, S., Peale, S. J., Rasio, F. A. 2010, ApJ, 725, 1995

Maxted, P. F. L., Anderson, D. R., Collier-Cameron, A., Gillon, M., Hellier, C. et al. 2010, PASP, 122, 1465

Nagasawa, M., Ida, S., Bessho, T. 2010, ApJ, 678, 498

O'Donovan, F. T., Charbonneau, D., Bakos, G. Á., Mandushev, G., Dunham, E. W. et al. 2007, ApJ, 663, L37

Pollacco D. L., et al. 2006, PASP, 118, 1407

Pollacco, D. L., Skillen, I., Collier-Cameron, A., Loeillet, B., Stempels, H. C. et al. 2008, MNRAS, 385, 1576

Pont, F., Moutou, C., Gillon, M., Udalski, A., Bouchy, F. et al. 2007, A&A, 465, 1069

Pringle, J. E. 1985, Interacting Binary Stars, Pringle, J. E. and Wade, R. A., Cambridge University Press, p. 1

Rutten, R. G. M. & Dhillon, V. S. 1996, CVs and Related Objects, Kluwer Academic Publ., 21-24

Sanchis-Ojeda, R., Winn, J. N., Marcy, G. W., Howard, A. W., Isaacson, H. et al. 2013, ApJ, 775, 54

Sasselov. D. D. 2008, Nature, 451, 29

Sato, B., Fischer, D. A., Henry, G. W., Laughlin, G., Butler, R. P. et al. 2005, ApJ, 633, 465

Sing, D. K., Lecavelier des Etangs, A., Fortney, J. J., Burrows, A. S, Pont, F. et al. 2013, MNRAS

Sirotkin, F. V. & Kim, W. T. 2009, ApJ, 698, 715

Smalley, B., Anderson, D. R., Collier-Cameron, A., Gillon, M., Hellier, C. et al. 2010, A&A, 520, A56

Snellen, I.A.G. and Albrecht, S. and de Mooij, E.J.W. & Poole, R.S. Le, 2008, A&A, 487, 357

Snellen, I. A. G., Koppenhoefer, J., van der Burg, R. F. J., Dreizler, S., Greiner, J. et al. 2009, A&A, 497, 545

Southworth, J. 2010, MNRAS, 408, 1689

Street, R. A., Simpson, E., Barros, S. C. C., Pollacco, D. L., Joshi, Y. et al. 2010, ApJ, 720, 337

Swift, D. C., Eggert, J. H., Hicks, D. G., Hamel, S., Caspersen, K. et al. 2012, ApJ, 744, 59

Szabó, Gy. M. & Kiss, L. L. 2011, ApJ, 727, L44

Tingley, B., Endl, M., Gazzano, J. C., Alonso, R., Mazeh, T. et al. 2011, A&A, 528, A97

Torres, G., Bakos, G. Á., Kovács, G., Latham, D. W., Fernández, J. M. et al. 2007, ApJ, 666, L121

Triaud, A. H. M. J., Collier Cameron, A., Queloz, D., Anderson, D. R., Gillon, M. et al. 2010, A&A, 524, A25

Watson, C. A. & Dhillon, V. S. 2001, MNRAS, 326, 67

Watson, C. A., Dhillon, V. S., Rutten, R. G. M., Schwope, A. D. 2003, MNRAS, 341, 129

Watson, C. A. & Dhillon, V. S. 2004, Astronomische Nachrichten, 325, 189

Wolszcan A. & Frail D. A. 1992, Nature, 355, 145

This preprint was prepared with the AAS LaTeX macros v5.2.

Table 2: Derived parameters for short-period hot-Jupiter exoplanets, with modified density values taking into account distortion due to tidal forces. Columns 1-6 and 8 are the parameters given in the corresponding reference (7). Column 9 is the adjusted density for the planet taking into account tidal distortion. Column 10 is the percentage difference between the two densities.

System	P(d)	M_S ($M_\odot$)	M_P (M_J)	R_P (R_J)	i (°)	Ref.	ρ_{sph}	ρ_{dis}	$\Delta\rho$
(1)	(2)	(3)	(4)	(5)	(6)	(7)	(8)	(9)	(10)
WASP-19	0.7888	0.97	1.168	1.386	79.4	[1]	0.438	0.392	12.00%
WASP-43	0.8134	0.58	1.78	0.93	82.6	[2]	2.210	2.160	2.18%
WASP-12	1.0914	1.35	1.41	1.79	83.1	[3]	0.240	0.222	10.95%
OGLE-TR-56	1.2119	1.17	1.29	1.30	78.8	[4]	0.587	0.571	2.85%
HAT-P-23*	1.2129	1.13	2.090	1.368	85.1	[5]	0.816	0.799	2.16%
TrES-3	1.3061	0.924	1.92	1.295	82.15	[6]	0.884	0.872	2.59%
Wasp-4	1.3382	0.93	1.250	1.34	89.47	[7]	0.520	0.502	3.39%
Qatar-1	1.4200	0.85	1.090	1.165	83.47	[8]	0.689	0.676	3.23%
OGLE-TR-113	1.4325	0.78	1.24	1.11	87.7	[9]	0.907	0.889	1.96%
Corot-1	1.5090	0.95	1.03	1.49	85.1	[10]	0.311	0.299	4.16%
Corot-14	1.5121	1.13	7.6	1.09	79.6	[11]	5.869	5.844	0.42%
WASP-5	1.6284	1.00	1.555	1.14	86.1	[7]	1.050	1.037	1.24%
OGLE-TR-132	1.6899	1.297	1.17	1.25	83.3	[12]	0.599	0.588	1.80%
Corot-2	1.7430	0.97	3.31	1.466	87.84	[13]	1.050	1.042	0.79%
WASP-3	1.8468	1.24	1.76	1.31	84.4	[14]	0.783	0.774	1.21%
WASP-48	2.1436	1.09	0.98	1.67	80.09	[15]	0.21	0.205	2.83%
WASP-2	2.1522	0.803	0.847	0.807	84.81	[12]	1.612	1.606	0.32%
HAT-P-7	2.2047	1.47	1.800	1.42	84.1	[16]	0.629	0.621	1.15%
HD189733	2.2186	0.840	1.15	1.15	85.78	[12]	0.756	0.747	1.17%
WASP-14	2.2438	1.211	7.341	1.28	84.32	[17]	3.500	3.490	0.10%
WASP-24	2.3412	1.184	1.071	1.30	83.64	[18]	0.487	0.481	1.21%
TrES-2	2.4706	0.98	1.198	1.169	84.15	[19]	0.750	0.747	0.44%
OGLE2-TR-L9	2.4855	1.52	4.5	1.61	79.8	[20]	1.078	1.074	0.38%
WASP-1	2.5200	1.243	0.860	1.48	88.0	[12]	0.265	0.258	2.67%
XO-2	2.6159	0.98	0.57	0.980	88.9	[21]	0.606	0.602	0.61%
GJ 436*	2.6439	0.459	0.0737	0.365	86.43	[12]	1.516	1.512	0.27%
WASP-32	2.7187	1.10	3.60	1.18	85.3	[22]	2.191	2.189	0.10%
WASP-26	2.7566	1.12	1.02	1.32	82.5	[23]	0.443	0.440	0.79%
HAT-P-16	2.7760	1.218	4.193	1.289	86.6	[24]	1.958	1.955	0.13%
HAT-P-5	2.7885	1.16	1.06	1.26	86.75	[25]	0.530	0.527	0.56%
HAT-P-30	2.811	1.242	0.711	1.34	83.6	[26]	0.295	0.292	1.08%
Corot-12	2.8280	1.078	0.917	1.44	85.48	[27]	0.309	0.303	1.25%
HD149026	2.8759	1.271	0.356	0.610	88.0	[12]	1.570	1.560	0.23%
HAT-P-3	2.8997	0.936	0.599	0.889	87.24	[28]	0.853	0.849	0.36%

* These planets have an appreciable eccentricity, with HAT-P-23 having e=0.106, and GJ436 having e=0.15, and therefore do not strictly satisfy the condition of orbital circularisation assumed by equation 1.

[1] Hellier et al. (2011a) [2] Hellier et al. (2011b) [3] Hebb et al. (2009) [4] Pont et al. (2007) [5] Bakos el al. (2011) [6] O'Donovan et al. (2007) [7] Triaud et al. (2010) [8] Alsubai et al. (2011) [9] Gillon et al. (2006) [10] Barge et al. (2008) [11] Tingley et al. (2011) [12] Southworth (2010) [13] Alonso et al. (2008) [14] Pollacco et al. (2008) [15] Enoch et al. (2011) [16] Lammer et al. (2009) [17] Joshi et al. (2009) [18] Street et al. (2010) [19] Christiansen et al. (2011) [20] Snellen et al. (2009) [21] Burke et al. (2007) [22] Maxted et al. (2010) [23] Smalley et al. (2010) [24] Buchhave et al. (2010) [25] Bakos et al. (2007) [26] Johnson et al. (2011) [27] Gillon et al. (2010) [28] Torres et al. (2007)